SEMARAK ILMU PUBLISHING

Journal of Advanced Research in Fluid Mechanics and Thermal Sciences

Journal homepage: https://semarakilmu.com.my/journals/index.php/fluid_mechanics_thermal_sciences/index
ISSN: 2289-7879

Significance of Melting Heat Transfer, Inclined Magnetic Field, and Thermal Radiation on the Dynamics of Williamson Nanofluid Above a Stretching Sheet

Anagandula Srinu[1,*], K. Sreeram Reddy[1]

[1] Department of Mathematics, University College of Science, Osmania University, Hyderabad-500007, Telangana, India

ARTICLE INFO

Article history:
Received 5 August 2023
Received in revised form 15 October 2023
Accepted 27 October 2023
Available online 15 November 2023

Keywords:
Williamson fluid; bvp4c; radiation; inclined magnetic field

ABSTRACT

This study investigates the melting heat transfer in MHD flow that occurs when the flow is past a stretched sheet. With the use of the boundary layer concept, a set of non-linear ODEs is derived from a system of PDEs of motion and energy. After transforming the non-linear ODEs and their boundary conditions into dimensionless form with the use of appropriate similarity conversions, the equations are then numerically solved by employing the MATLAB inbuilt solver bvp4c method in conjunction with the shooting methodology. Through the use of a variety of charts and tables, the authors analyze and describe in depth the effects that relevant factors have on a variety of flow fields. As melting factor (Me) increases, it is discovered that the effect of Me on fluid temperature and velocity distributions decreases. Williamson parameter and inclined magnetic profile are shown to have decreasing impact on velocity and momentum parameter. After that, the findings are compared with the earlier published findings in limited situations of the issue, and it is discovered that they are in exceptional specify with those findings.

1. Introduction

In engineering processes such as the extraction of thermoplastic sheets, metal drawing, paper manufacture, and glass-fiber production, boundary layer flow as well as heat transfer across a stretched sheet have been shown to have several uses, and as a result, are regarded to be crucial. During the process of manufacturing, a stretched sheet will engage in interactions with the surrounding fluid on both a thermal and mechanical level. Bejan and Khair [1] investigated the process of heat and mass transport in a porous media via the use of natural convection. The boundary-layer flow of a nanofluid was investigated by Khan and Pop [2] as it passed a stretching sheet. For vertically stretched sheets of permeability, and fluid dynamics in the MHD regime, Rashidi *et al.,* [3] investigated free convective heat and mass transfer with radiation and buoyancy effects. The MHD flow and heat transmission across a permeable stretched sheet under slip conditions were

* *Corresponding author.*
E-mail address: daruvusrinu@gmail.com

https://doi.org/10.37934/arfmts.111.1.4157

scrutinized by Hayat *et al.,* [4]. The movement of a Williamson fluid was investigated by Nadeem *et al.,* [5] who used a stretched sheet.

It is of great importance in contemporary metallurgy and metalworking to learn about the MHD movement of an electrically conducting fluid. In an electrical furnace, a magnetic field is used to fuse metals, and in a nuclear reactor, a magnetic field is used to cool the first wall by isolating the hot plasma from the wall, thereby cooling the wall. Concerning species diffusion, Pal and Mondal [6] study non-Darcy MHD mixed convective diffusion of species across a stretched sheet in an absorbent substance with several variables. The effects of a stretched sheet's slip on heat and mass transmission inside an MHD boundary layer were studied by Kumar [7]. Mixed convection and convective boundary conditions were investigated for the MHD Falkner-Skan flow by Masood *et al.,* [8]. The MHD boundary layer flow caused by an exponentially stretched sheet with radiation impact was investigated by Ishak [9]. Krishnamurthy *et al.,* [10] investigated how chemical reaction influences MHD boundary layer flow and melting heat transmission of Williamson nanofluid in porous media.

None of the prior studies have considered the role radiation plays in influencing the flow and transfer of heat. It is common knowledge that radiative heat transfer flow plays a crucial role in the engineering of safe and effective machinery, nuclear power plants, gas turbines, and a wide range of aerospace propulsion systems. High-temperature space technologies and processes rely heavily on understanding how heat radiation affects forced and free convection flow. Megahed [11] investigated the Williamson flow of a viscous dissipating and thermally radiating fluid caused by a nonlinearly expanding sheet. Powell-Eyring fluid with dual convection and heat production effects was deliberate numerically by Malik *et al.,* [12] at the stationary point of MHD heat and solutal stratification flow. MHD Williamson nanofluid flow with heat radiation and chemical reaction was investigated by Patil *et al.,* [13]. Using nonlinear mixed convection, velocity slips, and radiation, Das *et al.,* [14] analyzed the flow of a Williamson nanofluid in an MHD fluid through a stretched sheet. Non-linear heat radiation and binary chemical reaction were studied by Sharma *et al.,* [15] to see how they affected the flow of a Williamson nanofluid via a linearly extending sheet.

Williamson postulated a non-Newtonian fluid with shear thinning properties, and this fluid is presented here. He claims that this fluid plays a crucial role in differentiating plastic from viscous flow. The flexible nature of the dispersion is represented in the momentum-controlling equation by a fluctuating apparent viscosity. The pseudoplastic fluid behavior that this non-Newtonian fluid enables has numerous practical uses in industry.

Heat transfer properties of the MHD flow of Williamson nanofluid across an exponentially permeable stretched curved surface with varying thermal conductivity were investigated by Ahmed *et al.,* [16]. Bouslimi *et al.,* [17] studied the several impacts on the stretching of a sheet of MHD Williamson nanofluid flowing over a porous material. Using an exponentially extending surface, Kumar *et al.,* [18] investigated the MHD movement of a nanofluid created by Williamson in the context of chemical reaction and radiation. Research using numerical methods into the MHD peristaltic movement of a Williamson nanofluid contained inside an endoscope with partial slip and wall features were provided by Hayat *et al.,* [19]. Williamson nanofluid flow, heat transfer, and mass transfer across a stretched sheet were all investigated by Srinivasulu and Goud [20]. Williamson nanofluid MHD flow with heat and mass transport across a stretched sheet in a porous media was investigated by Shawky *et al.,* [21]. Boundary layer flow of Williamson fluid including chemically reactive species was investigated by Khan *et al.,* [22] utilizing the scaling modification and homotopy assessment approach. Mass and Heat transmission in a Williamson nanofluid with a porous media was studied by Reddy *et al.,* [23], specifically the influence of flow factors on MHD boundary layer flow. Over an exponentially permeable stretched surface, Li *et al.,* [24] study the heat and mass transport in an MHD Williamson nanofluid. Abbas *et al.,* [25] investigated the impact of heat production and dissipation on MHD Williamson nanofluid flow and heat transmission across a non-linear elastic sheet placed in a porous media.

The phenomena of melting and solidification are very important to the process of developing new technologies. The phenomena of melting that occur during the solid–liquid phase transition have a wide range of applications, some of which include welding, crystal formation, thermal protection, heat transmission, and the melting of permafrost. Semiconductor material preparation is another one of these applications. Melting heat transfer was investigated by Hayat *et al.,* [26] in the context of stagnation point flow of Powell–Eyring fluid. Dadheech *et al.,* [27] investigated the fluid flow and heat transfer caused by a non-linear heat source passing through a conductive melting surface. The MHD micropolar fluid flow across a stretched surface was investigated by Sharma *et al.,* [28], who also looked at the melting and slide effect. Mabood *et al.,* [29] investigated the effects of radiation on stagnation point flow with melting heat transfer and second order slip. Some of the researchers studied the different aspects of various flow fields [30-35].

This article investigates the effects of Williamson hydromagnetic fluid flowing past a stretching sheet through thermal radiation with a heat sink/source. Joule heating, viscous diffusion, thermal radiation effect, and inclined magnetic parameters are also considered. The transformed governing partial differential equations have been solved numerically using the bvp4c technique. The effect of relevant flow parameters on momentum, and thermal behavior, such as the skin friction factor and the rate of thermal is investigated and published with the help of graphical and tabular representations. The findings of these studies are used in a wide variety of engineering and metallurgical applications, as well as to enhance the performance of systems that transport thermal fluids.

2. Basic Equations

Consider a linearly stretched flow, which comprises a 2-D steady flow of Williamson fluid. Flow is being held to $y > 0$. It takes an angle γ with the x-axis and applies the magnetic field to the fluid movement vertically. T_w, T_∞ are assumed that they are respectively represented as ambient fluid temperature, Williamson fluid flow at the sheet of the concentration and temperature. The flow model of the problem is like Figure 1 and the velocity of the stretching sheet is $u_w(x) = ax$ and ignored the induced magnetic field and assessed to be knowingly lower compared to the applied magnetic field extra.

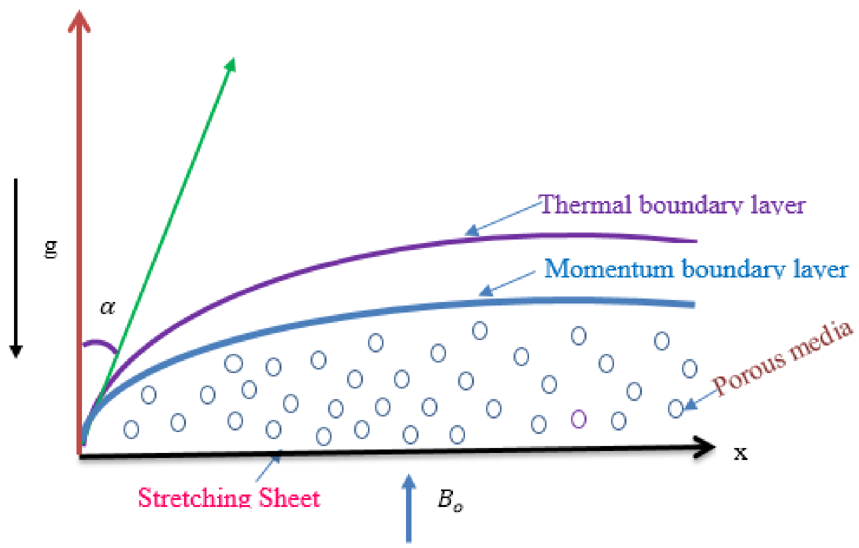

Fig. 1. Flow geometry

The Williamson fluid type for this assumption can be taken by Srinivasulu and Goud [20] as considered. For the tensor of Cauchy stress, s it is defined as;

$$s = -pl + \tau_1,$$

$$s = -pl = \left(\mu_\infty + \frac{\mu_0 - \mu_\infty}{1 - \Gamma\gamma}\right) A_1$$

Here Γ >0 is the time constant then γ is given as $\gamma = \sqrt{\frac{\pi}{2}}, \pi = trace(A_1^2)$

$$\sqrt{\left[\left(\frac{\partial u}{\partial x}\right)^2 + \frac{1}{2}\left(\frac{\partial u}{\partial y} + \frac{\partial v}{\partial x}\right)^2 + \left(\frac{\partial v}{\partial y}\right)^2\right]}$$

We considered only the case $\mu_\infty = 0$ and Γ <1.

Then, we get $\tau_1 = [\mu_0 A_1 (1 - \Gamma)^{-1}] \; or \; \tau_1 = [\mu_0 A_1 (1 + \Gamma)]$.

The governing equations are:

$$\frac{\partial u}{\partial x} + \frac{\partial v}{\partial y} = 0 \tag{1}$$

$$u\frac{\partial u}{\partial x} + v\frac{\partial u}{\partial y} = v\frac{\partial^2 u}{\partial y^2} + \sqrt{2}v\Gamma\frac{\partial u}{\partial y}\frac{\partial^2 u}{\partial y^2} - \frac{\sigma B_0^2 u}{\rho_f}\sin^2(\gamma) - \frac{\mu}{\rho k^*}u \tag{2}$$

$$u\frac{\partial T}{\partial x} + v\frac{\partial T}{\partial y} = \frac{K}{(\rho C_p)_f}\left(\frac{\partial^2 T}{\partial y^2}\right) + \frac{1}{(\rho C_p)_f}\frac{16\sigma^* T_\infty^2}{3K^*}\frac{\partial^2 T}{\partial y^2} + \frac{\sigma B_0^2}{(\rho C_p)_f}u^2 + \frac{v}{C_p}\left[\left(\frac{\partial u}{\partial y}\right)^2 + \sqrt{2}\Gamma\left(\frac{\partial u}{\partial y}\right)^3\right] + Q(T - T_\infty) \tag{3}$$

The initial boundary conditions are,

$$\left.\begin{aligned} u_x = u = ax, v = 0, T = T_w,\; k^{**}\left(\frac{\partial T}{\partial y}\right) = \rho\{\lambda + C_s(T_w - T_o)\}v(x,y) \;\; as\; y \to 0 \\ u = 0, T = T_\infty,\; as\; y \to \infty \end{aligned}\right\} \tag{4}$$

The variable similarity transformation is as follows,

$$\psi = \sqrt{av}xf(\eta),\; \eta = y\sqrt{\frac{a}{v}},\; \theta(\eta) = \frac{T - T_\infty}{T_w - T_\infty} \tag{5}$$

Where $f(\eta), \theta(\eta)$ are the non-dimensional stream, velocity, and temperature functions respectively. Use Eq. (4) and Eq. (5) in nonlinear governing Eq. (1) to Eq. (3), then we get ODEs as:

$$f'''(1 + \lambda f'') + ff'' - f'^2 - f'(M\sin^2(\alpha) + Kp) = 0 \tag{6}$$

$$(1 + R)\theta'' + \Pr[f\theta' + Ec(f''^2 + Wef''^3 + Mf'^2) + Q\theta] = 0 \tag{7}$$

Consequently, the associative boundary restrictions [9]

$$\left.\begin{array}{c} f'(0) = 1,\ Prf(0) + Me\,\theta'(0) = 0, \theta(0) = 1,\ at\,\eta = 0 \\ f'(\infty) = 0,\ \theta(\infty) = 0, as\,\eta \to \infty \end{array}\right\} \tag{8}$$

Here the governing constraints are defined as:

$$M = \frac{\sigma B_0^2}{\rho_f a},\ Pr = \frac{K}{(\rho C_p)_f}, \lambda = \sqrt{\frac{2a}{v}}ax\Gamma\,, Kp = \frac{v}{k^*}$$

$$R = \frac{16\sigma^* T_\infty^3}{3K^* K}, We = x\Gamma\sqrt{\frac{2a^3}{v}}\,, Ec = \frac{u_w^2}{C_p(T_w - T_\infty)}, \tag{9}$$

Here are several definitions for the physical dimensions of Nusselt number and skin friction:

$$Re_x^{\frac{1}{2}} C_{fx} = \left(1 + \frac{\lambda}{2} f''(0)\right) f''(0), Re_x^{-\frac{1}{2}} Nu_x = -(1 + R)\theta'(0) \tag{10}$$

Here $Re_x = \frac{u_w x}{v}$ is taken as Reynolds number.

3. Solution of the Problem

The nonlinear ODEs (6-8) and the boundary limits (9) are both integrated with the assistance of the MATLAB function known as bvp4c. This is accomplished by first changing the collection of ODEs to first-order ODEs by sequential replacements. Let's just let $\xi = [U\ U'\theta\ \theta'\ ]^T$ which provides

Step 1: A first-order set of equations has been established:

$$\frac{d}{d\eta}\begin{pmatrix} \xi(1) \\ \xi(2) \\ \xi(3) \\ \xi(4) \\ \xi(5) \end{pmatrix} = \begin{pmatrix} \xi(2) \\ -\frac{\left(\xi(1)\xi(3) - \left(Msin^2(\alpha) + Kp\right)\xi(1) - \xi(1)^2\right)}{(1 + \lambda\xi(3))} \\ \xi(4) \\ \frac{-Pr\left((\xi(4)\xi(1) + \mathrm{Ec}\left(\xi(2)\right)^2 + \mathrm{We}\,\xi(3)^2 + \mathrm{M}\,\xi(3)^2 + Q\xi(4)\right)}{(1 + R)} \end{pmatrix}$$

Step 2: To do the numerical solution, we use the bvp4c solver that comes pre-installed in MATLAB and set the far area boundary requirement to a fixed value that makes sense for our purposes. This is seen as a problem associated with boundary values, i.e., $\eta \to \infty$ say $\eta \to 10$.

Initial constraints include the following:

$$\begin{pmatrix} \xi a(2) \\ \xi a(1) \\ \xi a(4) \\ \xi b(2) \\ \xi b(4) \end{pmatrix} = \begin{pmatrix} 1 \\ -Me\xi a(5)/Pr \\ 1 \\ 0 \\ 0 \end{pmatrix}$$

A value of $\eta = 0.01$ is used for the scaling factor, and the conditions for convergence are specified to the fifth decimal place.

The asymptotic stability of the boundary limitation (9) was determined to be 10^{-6}. In boundary layer evaluation, it is common practice to set $\eta_\infty = 10$.

4. Numerical Code Validation

It is possible to see from Table 1 that as the values of the Prandtl number upsurge, the values of $-\theta'(0)$ also rise. Through numerical analysis, we find that our finding agrees very well with the restrictive results provided by researchers Khan *et al.,* [22]. It demonstrates the precision expected and a verification code is thus allowed.

Table 1
Comparison of values of $-\theta'(0)$ with previous results when $\lambda = R = Ec = M = Kp = Me = 0$

Pr	Khan *et al.,* [22]	Present study
0.7	0.4539	0.4539
2	0.9113	0.9113
7	1.8954	1.8954

5. Result and Discussion

The effect of different parameters like inclined angle, Williamson parameter, heat sink/source, Prandtl number, magnetic parameter, Weissenberg number, thermal radiation, and Eckert number on momentum and thermal parameters is graphically discussed. In Figure 2 scrutinizing the consequence of a magnetic profile on the momentum parameters, a drag force is known as the Lorentz force and it is improved by administrating the magnetic field because this boundary layer surface is attracted towards the velocity and hence the thickness lowers as magnetic strength is higher.

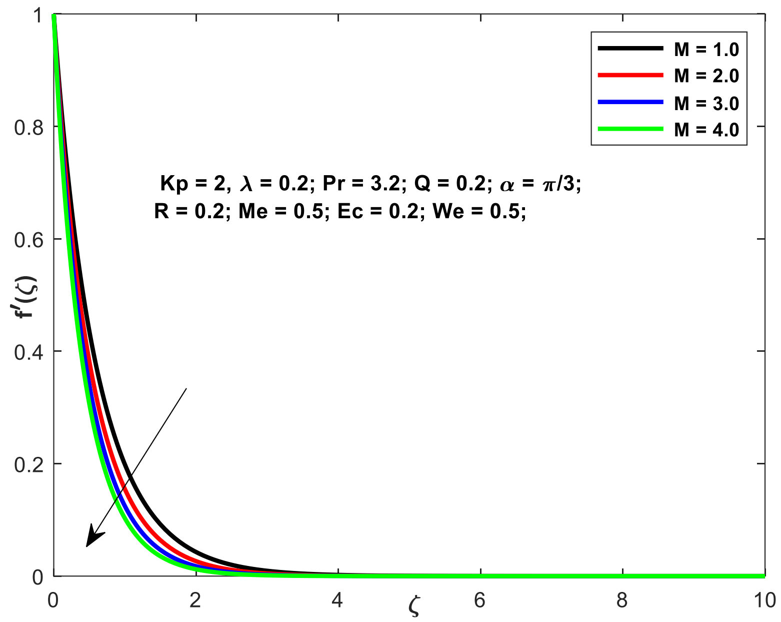

Fig. 2. Velocity $(f'(\zeta))$ vs Magnetic parameter

Figure 3 elucidates the attributes of magnetic factor (M) versus θ(η). Increasing (M) has the expected impact of increasing the temperature fields. As a result, with larger values of (M), both the width of the momentum and the temperature boundary layer diminish.

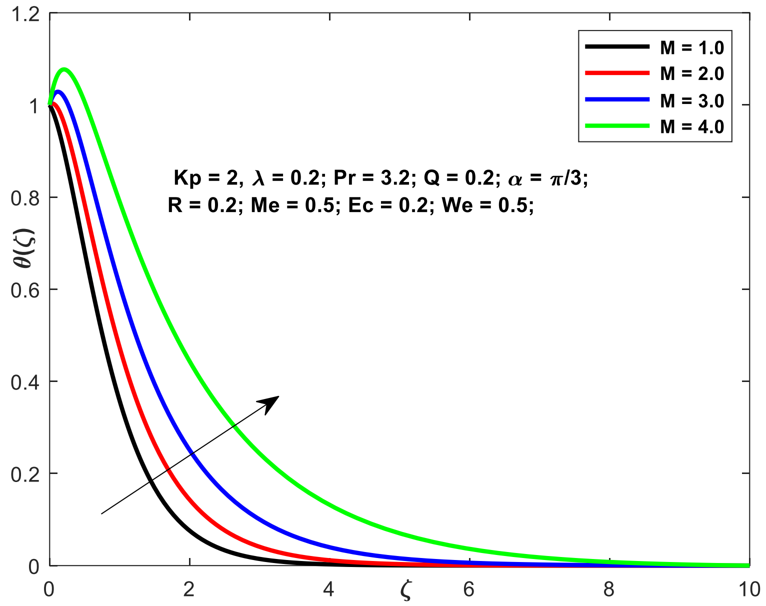

Fig. 3. Temperature$\theta(\zeta)$ vs Magnetic parameter M

The consequence of the permeability component is seen in Figure 4, where it is seen that the velocity profile rises for large values of Kp. It's now shown that a larger Kp results in a wider momentum boundary layer.

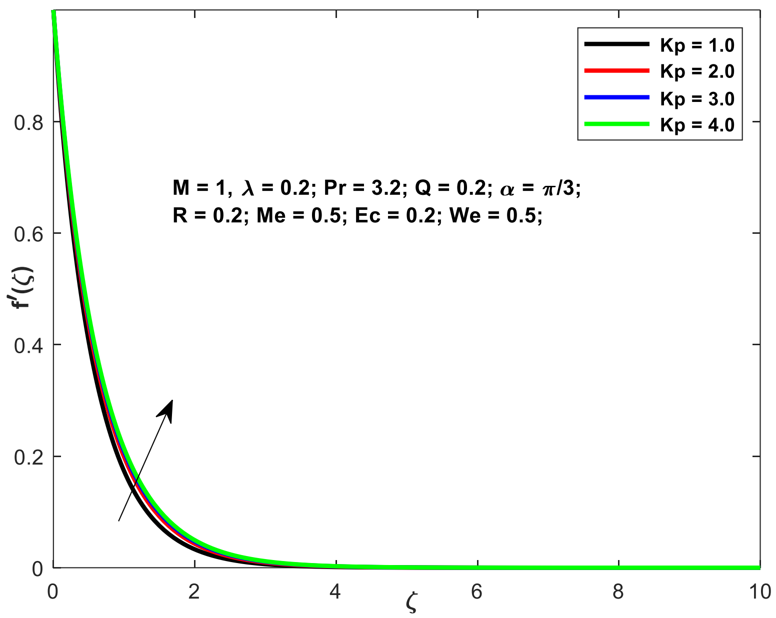

Fig. 4. Velocity $f'(\zeta)$ vs permeability Kp

The influence of the permeability parameter(Kp) on the fluid temperature is seen in Figure 5. It has been observed that when the Kp parameter is iterated in a positive direction, the temperature profile displays a declining attitude.

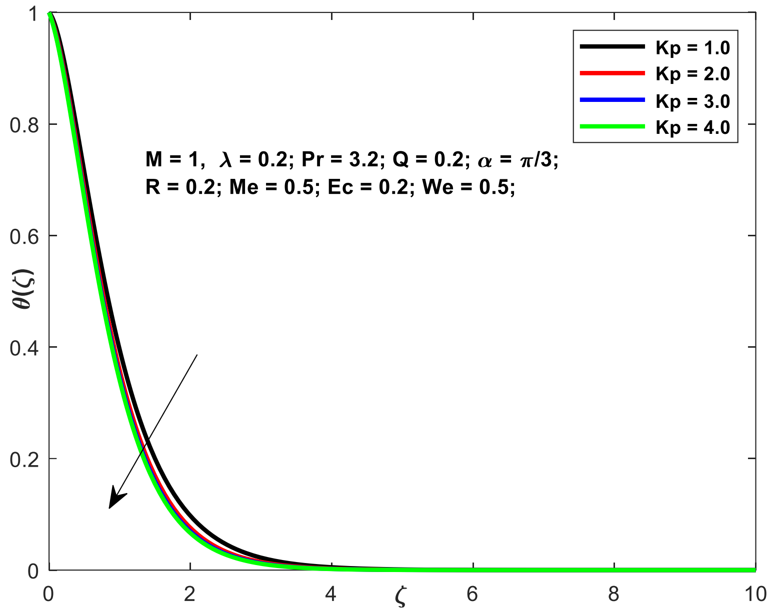

Fig. 5. Temperature $\theta(\zeta)$ vs Kp

The results of the Eckert number Ec's effect on the velocity profile are shown in Figure 6. The velocity and depth of the boundary layer both rise with higher amounts of Ec.

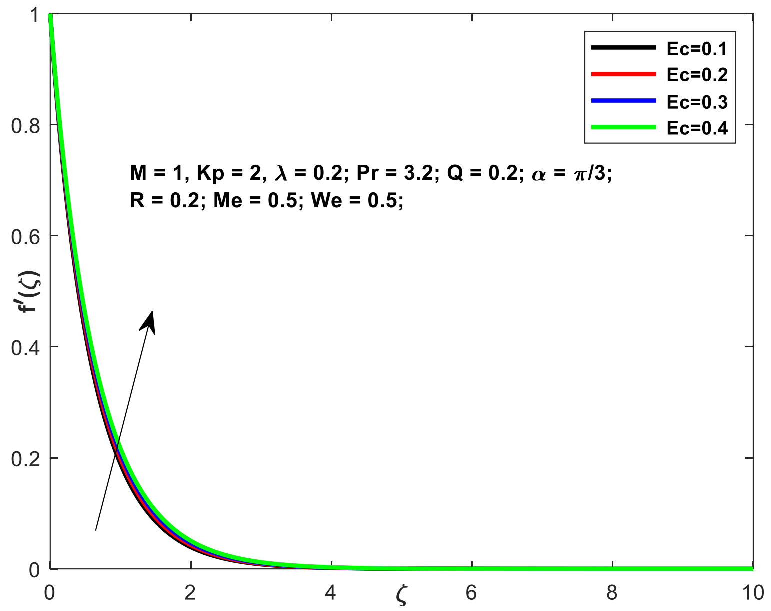

Fig. 6. Velocity $f'(\zeta)$ vs Eckert number Ec

Figure 7 displays the relationship between the fluid's velocity and the angle of inclination. It's been observed that the angle of an object's inclination is inversely proportional to its velocity curve. When α is increased, the velocity pattern flattens out. Increasing the angle of inclination on α the x-axis diminishes the pull of gravity, slowing the flow of fluid inside the boundary layer.

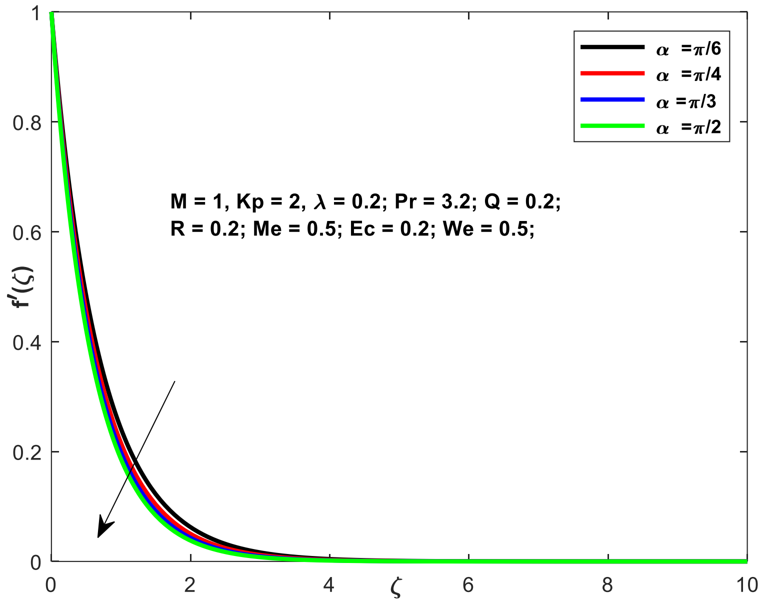

Fig. 7. Velocity $f'(\zeta)$ vs Angle of inclination α

A correlation between the fluid's temperature and the angle of α is seen in Figure 8. It has been observed that when the value of inclination α is increased, the pattern of temperature also rises. This is because, as the inclination α about the x-axis rises, the efficacy of gravity rises, and the rise in temperature pattern is a direct result of this.

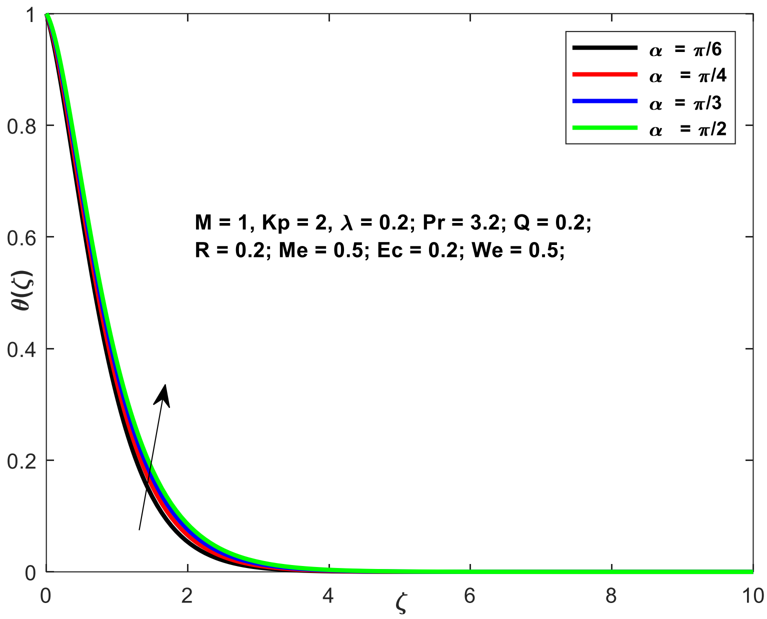

Fig. 8. Temperature $\theta(\zeta)$ vs Angle of inclination α

As seen in Figure 9, the influence of the Prandtl number(Pr) reduces the temperature gradient. Since the Pr number inversely correlates to thermal conductivity, extending it will reduce the rate at which heat is transferred through the fluid, resulting in a cooler fluid and a more uniformly dispersed thermal boundary layer. Overestimate in the boundary layer of heat occurs with large Pr, making the situation harder to comprehend. We use the concept of a heat sink, which restores a more normal temperature, to prevent this kind of overshoot.

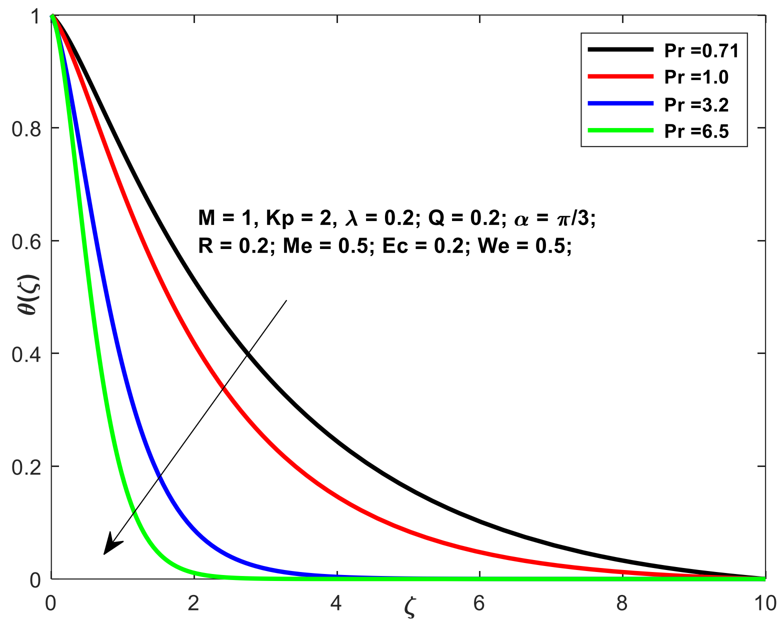

Fig. 9. Temperature $\theta(\zeta)$ vs Prandtl number Pr

Figure 10 depicts how the Eckert number (Ec) influences the temperature gradients. The Ec value shows the efficiency with which function over viscous fluid tension converts kinetic energy into internal energy. A rise in the viscous dissipation factor is shown to increase energy.

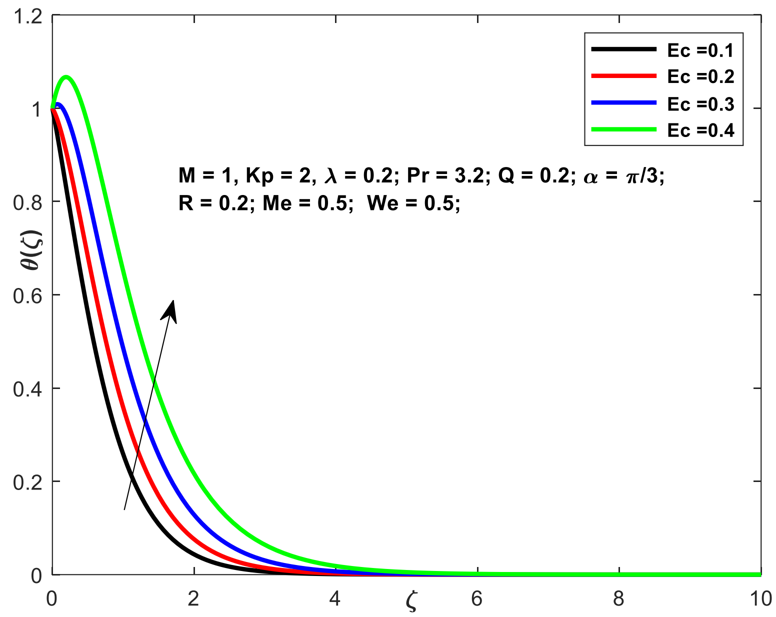

Fig. 10. Temperature $\theta(\zeta)$ vs Ec

Figure 11 provides a source for the fluid velocity attitude towards the Williamson factor(λ), and it can be seen that when λ is increased, the velocity profile diminishes. As λ increases, the particles' relaxation time grows, raising their viscosity and therefore creating resistance to the fluid movement, which slows down the particles' velocity.

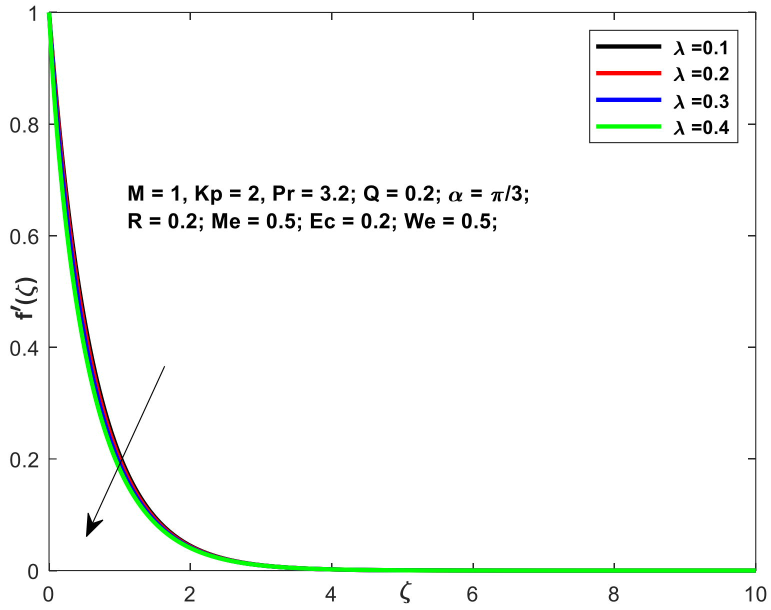

Fig. 11. Velocity $f'(\zeta)$ vs Williamson factor λ

The influence of the Williamson component (λ) on the temperature curve is seen in Figure 12. As λ rises, the temperature distribution also rises, according to the evidence. The average temperature rises as the heat production parameter is given positive values to play a more substantial role in the process.

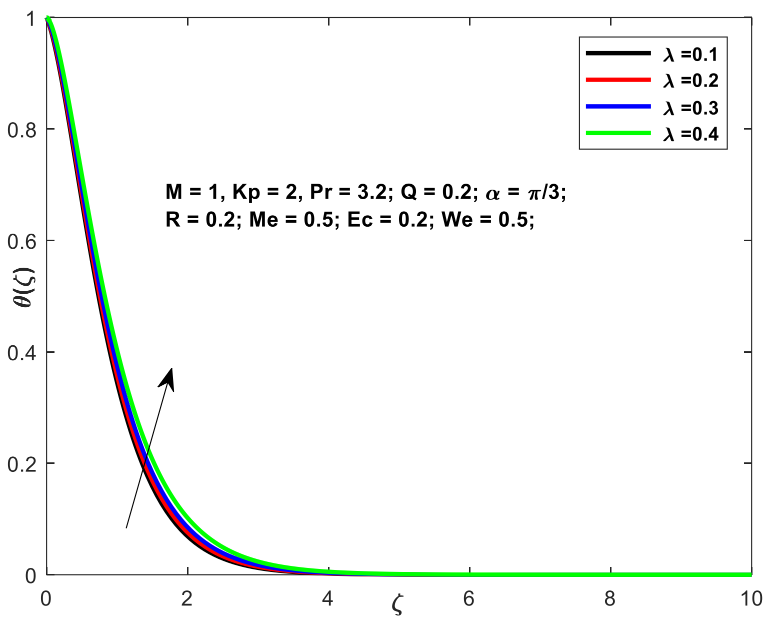

Fig. 12. Temperature $\theta(\zeta)$ vs Williamson factor λ

The impact of Weinssenberg (We) on thermal distributions is seen in Figure 13. Results show that higher values of We improve temperature profiles, leading to a larger boundary layer.

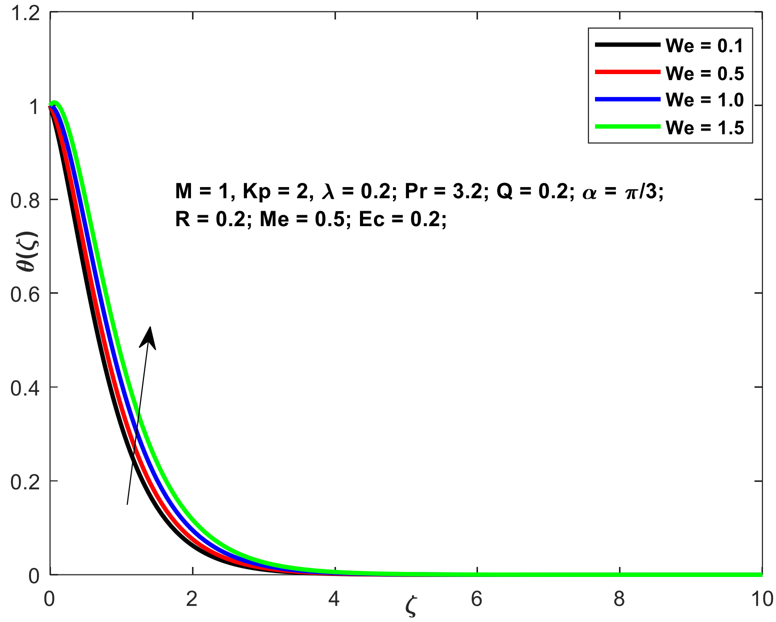

Fig. 13. Temperature $\theta(\eta)$vs Weinssenberg We

Figure 14 shows the velocity after being exposed to the Weissenberg. It demonstrates that raising the Weissenberg number improves the profile of $f'(\eta)$. For larger estimates of We, it is significant to note that the width of the momentum border layer increases.

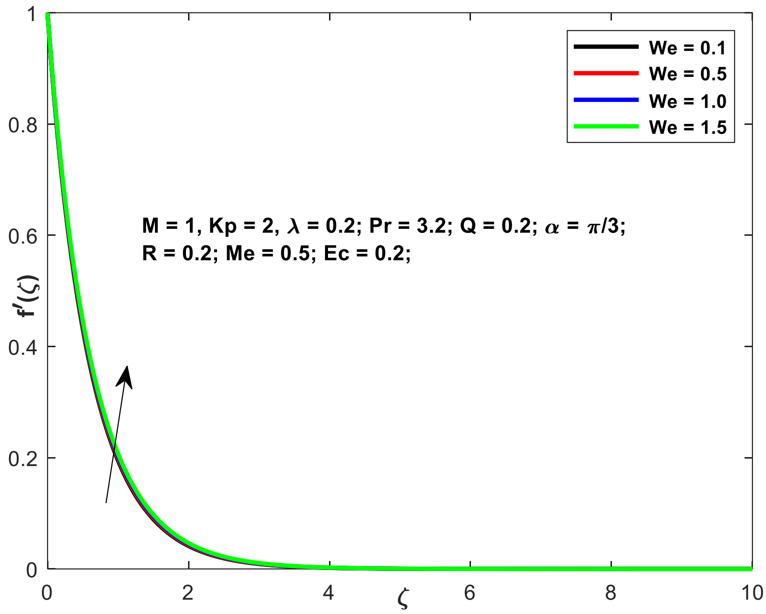

Fig. 14. Velocity $f'(\zeta)$ vs Weinssenberg We

After being subjected to the heat source, the temperature rises as shown in Figure 15. Increasing the heat source component leads to higher temperatures, as seen in the figure.

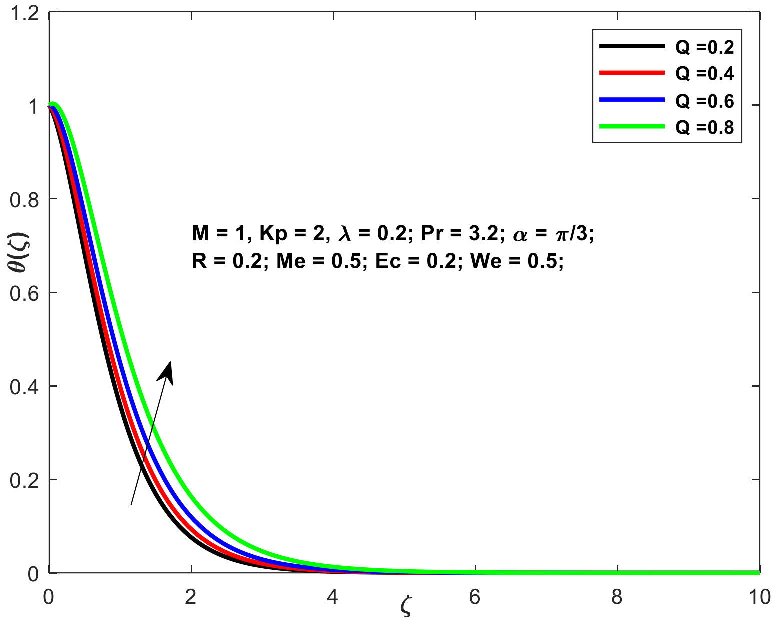

Fig. 15. Temperature $\theta(\zeta)$ vs Heat source Q

Using the radiation parameter(R), the consequences of R on the temperature profile is seen in Figure 16. It turns out that when R rises, the temperature curves improve noticeably, as more heat is supplied to the fluid, raising both the thermal and temperature boundary layer width.

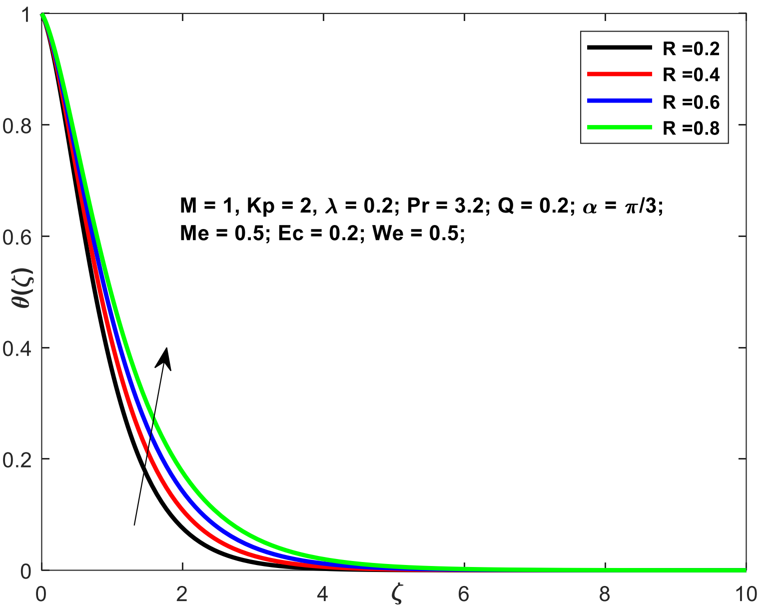

Fig. 16. Temperature $\theta(\zeta)$ vs Thermal radiation R

Figure 17 and Figure 18 depict the impact of the melting factor (Me) on the velocity and temperature of the fluid, respectively. It is perceived that the velocity and temperature distributions drop as Me rises.

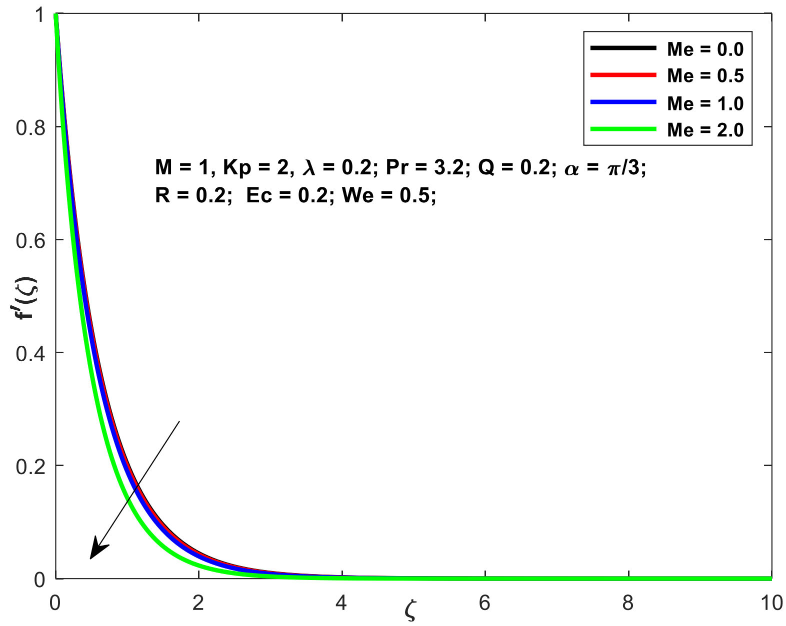

Fig. 17. Velocity $f'(\zeta)$ vs Melting parameter Me

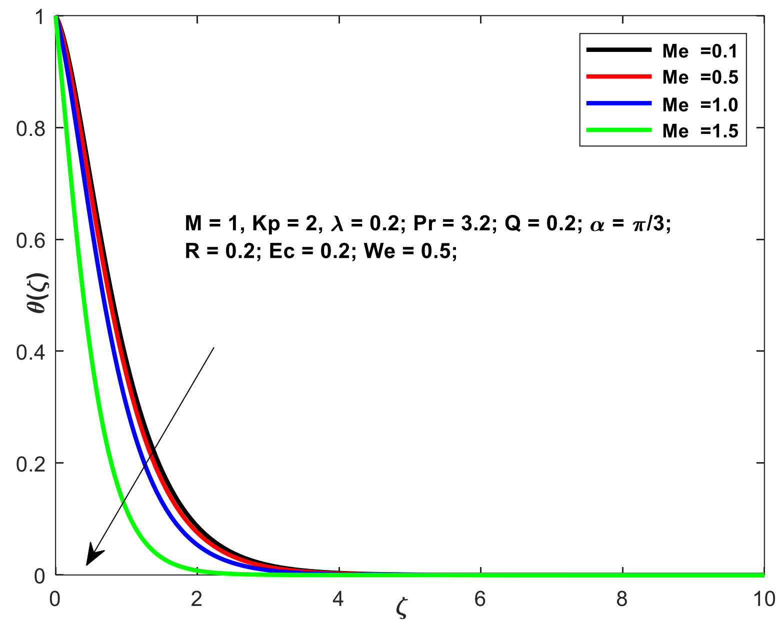

Fig. 18. $\theta(\zeta)$ vs Me

Table 2 illustrates the dependence of $C_f(Re_x)^{\frac{1}{2}}$, & $Nu_x(Re_x)^{-\frac{1}{2}}$ on M, Kp, L, and Me. The table indicates that when M, L, and Me grow, the friction factor falls, but Kp, α increases. Nusselt number goes down as M, L, and Me go larger but up when parameter Kp, α gets bigger, as seen in the table.

Table 2

The variation of $M, \lambda, Me, Kp, \alpha$ on $C_f(Re_x)^{\frac{1}{2}}, Nu_x(Re_x)^{-\frac{1}{2}}$ and $Sh_x(Re_x)^{-\frac{1}{2}}$ with fixed $Pr = 3.2; Q = 0.2;\ R = 0.2;\ Ec = 0.2;\ We = 0.5$

M	Kp	λ	α	Me	$f''(0) + \frac{\lambda}{2} f''(0)^2$	$-\left(1 + \frac{4}{3}R\right)\theta'(0)$
1	2	0.2	$\pi/3$	0.5	-1.927146	0.319796
2					-2.276872	-0.203874
3					-2.602057	-0.680693
1	3				-1.861316	0.374957
	4				-1.827858	0.402862
	2	0.3			-2.247086	0.227556
		0.4			-2.556781	0.069543
		0.2	$\pi/4$		-1.817642	0.411363
			$\pi/6$		-1.668187	0.534586
				0.7	-1.947267	0.371142
				0.9	-1.975954	0.444291

Table 3 shows the change in $C_f(Re_x)^{\frac{1}{2}}, \& \ Nu_x(Re_x)^{-\frac{1}{2}}$ as a function of $Pr,\ R,\ Ec,\ We$, and Q. The values of Pr, R, Ec, We, and Q in the table indicate an increase in the skin friction coefficient. According to the data in the table, when Ec, We, and Q go up, the Nusselt number goes down, but the Pr, R parameter goes up.

Table 3

The variation of $Pr. R, Ec, We$, and Q on $C_f(Re_x)^{\frac{1}{2}}, and\ Nu_x(Re_x)^{-\frac{1}{2}}$ with fixed $M = 1;\ Kp = 2; \lambda = 0.2;\ \alpha = \pi/3;\ ;\ Me = 0.5$

Pr	R	Ec	We	Q	$f''(0) + \frac{\lambda}{2} f''(0)^2$	$-\left(1 + \frac{4}{3}R\right)\theta'(0)$
3.2	0.2	0.2	0.5	0.2	-1.927146	0.319796
1					-1.956382	0.190378
0.71					-1.963520	0.150650
3.2	0.4				-1.925310	0.364883
	0.6				-1.923451	0.401869
	0.2	0.3			-1.862992	-0.336476
		0.4			-1.802834	-0.980158
		0.2	0.7		-1.914370	0.191461
			0.9		-1.901966	0.065761
			0.5	0.4	-1.913404	0.181715
				0.6	-1.897469	0.019923

6. Conclusion

The current study is to analyze and focus on the influence of melting and heat source variables on Williamson fluid flow over a stretched surface with considerations of an inclined magnetic field. Using shooting techniques, numerical solutions are computed. The following important keys are:

(i) The fluid velocity and the temperature upsurge with an enhancement of the parameters M, Ec, We.
(ii) Temperature profile upsurges with the escalation of $Q\ and\ R$.
(iii) Velocity increases and the temperature drops with the impact of enhancing the value of Kp.
(iv) Increasing of γ velocity profile decreases and the temperature decreases.
(v) The velocity profile declines and the temperature upsurges as an enhancement of λ .

(vi) Enhance of melting Parameter (Me), velocity curve as well as the temperature decreases.
(vii) Temperature decreases Pr rises.

References

[1] Bejan, Adrian, and Khairy R. Khair. "Heat and mass transfer by natural convection in a porous medium." *International Journal of Heat and Mass Transfer* 28, no. 5 (1985): 909-918. https://doi.org/10.1016/0017-9310(85)90272-8

[2] Khan, W. A., and I. Pop. "Boundary-layer flow of a nanofluid past a stretching sheet." *International Journal of Heat and Mass Transfer* 53, no. 11-12 (2010): 2477-2483. https://doi.org/10.1016/j.ijheatmasstransfer.2010.01.032

[3] Rashidi, Mohammad Mehdi, Behnam Rostami, Navid Freidoonimehr, and Saeid Abbasbandy. "Free convective heat and mass transfer for MHD fluid flow over a permeable vertical stretching sheet in the presence of the radiation and buoyancy effects." *Ain Shams Engineering Journal* 5, no. 3 (2014): 901-912. https://doi.org/10.1016/j.asej.2014.02.007

[4] Hayat, T., M. Qasim, and S. Mesloub. "MHD flow and heat transfer over permeable stretching sheet with slip conditions." *International Journal for Numerical Methods in Fluids* 66, no. 8 (2011): 963-975. https://doi.org/10.1002/fld.2294

[5] Nadeem, S., S. T. Hussain, and Changhoon Lee. "Flow of a Williamson fluid over a stretching sheet." *Brazilian Journal of Chemical Engineering* 30 (2013): 619-625. https://doi.org/10.1590/S0104-66322013000300019

[6] Pal, Dulal, and Hiranmoy Mondal. "MHD non-Darcy mixed convective diffusion of species over a stretching sheet embedded in a porous medium with non-uniform heat source/sink, variable viscosity and Soret effect." *Communications in Nonlinear Science and Numerical Simulation* 17, no. 2 (2012): 672-684. https://doi.org/10.1016/j.cnsns.2011.05.035

[7] Kumar, B. Rushi. "MHD boundary layer flow on heat and mass transfer over a stretching sheet with slip effect." *Journal of Naval Architecture and Marine Engineering* 10, no. 2 (2013): 109-118. https://doi.org/10.3329/jname.v10i2.16400

[8] Masood, Khan, Ramzan Ali, and Azeem Shahzad. "MHD Falkner-Skan flow with mixed convection and convective boundary conditions." *Walailak Journal of Science and Technology (WJST)* 10, no. 5 (2013): 517-529.

[9] Ishak, Anuar. "MHD boundary layer flow due to an exponentially stretching sheet with radiation effect." *Sains Malaysiana* 40, no. 4 (2011): 391-395.

[10] Krishnamurthy, M. R., B. C. Prasannakumara, B. J. Gireesha, and Rama Subba Reddy Gorla. "Effect of chemical reaction on MHD boundary layer flow and melting heat transfer of Williamson nanofluid in porous medium." *Engineering Science and Technology, an International Journal* 19, no. 1 (2016): 53-61. https://doi.org/10.1016/j.jestch.2015.06.010

[11] Megahed, Ahmed M. "Williamson fluid flow due to a nonlinearly stretching sheet with viscous dissipation and thermal radiation." *Journal of the Egyptian Mathematical Society* 27, no. 1 (2019): 12. https://doi.org/10.1186/s42787-019-0016-y

[12] Malik, M. Y., S. Bilal, and M. Bibi. "Numerical analysis for MHD thermal and solutal stratified stagnation point flow of Powell-Eyring fluid induced by cylindrical surface with dual convection and heat generation effects." *Results in Physics* 7 (2017): 482-492. https://doi.org/10.1016/j.rinp.2016.12.025

[13] Patil, Vishwambhar S., Pooja P. Humane, and Amar B. Patil. "MHD Williamson nanofluid flow past a permeable stretching sheet with thermal radiation and chemical reaction." *International Journal of Modelling and Simulation* 43, no. 3 (2023): 185-199. https://doi.org/10.1080/02286203.2022.2062166

[14] Das, M., B. Kumbhakar, and J. Singh. "Analysis of unsteady MHD Williamson nanofluid flow past a stretching sheet with nonlinear mixed convection, thermal radiation and velocity slips." *Journal of Computational Analysis & Applications* 30, no. 1 (2022): 176-195.

[15] Sharma, Ram Prakash, S. R. Mishra, Seema Tinker, and B. K. Kulshrestha. "Effect of non-linear thermal radiation and binary chemical reaction on the Williamson nanofluid flow past a linearly stretching sheet." *International Journal of Applied and Computational Mathematics* 8, no. 4 (2022): 171. https://doi.org/10.1007/s40819-022-01362-w

[16] Ahmed, Kamran, Tanvir Akbar, Taseer Muhammad, and Metib Alghamdi. "Heat transfer characteristics of MHD flow of Williamson nanofluid over an exponential permeable stretching curved surface with variable thermal conductivity." *Case Studies in Thermal Engineering* 28 (2021): 101544. https://doi.org/10.1016/j.csite.2021.101544

[17] Bouslimi, Jamal, M. Omri, R. A. Mohamed, K. H. Mahmoud, S. M. Abo-Dahab, and M. S. Soliman. "MHD Williamson nanofluid flow over a stretching sheet through a porous medium under effects of joule heating, nonlinear thermal radiation, heat generation/absorption, and chemical reaction." *Advances in Mathematical Physics* 2021 (2021). https://doi.org/10.1155/2021/9950993

[18] Kumar, P. B., B. J. Gireesha, R. S. R. Gorla, and B. Mahanthesh. "Magnetohydrodynamic flow of Williamson nanofluid due to an exponentially stretching surface in the presence of thermal radiation and chemical reaction." *Journal of Nanofluids* 6, no. 2 (2017): 264-272. https://doi.org/10.1166/jon.2017.1317

[19] Hayat, Tasawar, Aqsa Saleem, Anum Tanveer, and Fuad Alsaadi. "Numerical study for MHD peristaltic flow of Williamson nanofluid in an endoscope with partial slip and wall properties." *International Journal of Heat and Mass Transfer* 114 (2017): 1181-1187. https://doi.org/10.1016/j.ijheatmasstransfer.2017.06.066

[20] Srinivasulu, Thadakamalla, and B. Shankar Goud. "Effect of inclined magnetic field on flow, heat and mass transfer of Williamson nanofluid over a stretching sheet." *Case Studies in Thermal Engineering* 23 (2021): 100819. https://doi.org/10.1016/j.csite.2020.100819

[21] Shawky, Hameda M., Nabil T. M. Eldabe, Kawther A. Kamel, and Esmat A. Abd-Aziz. "MHD flow with heat and mass transfer of Williamson nanofluid over stretching sheet through porous medium." *Microsystem Technologies* 25 (2019): 1155-1169. https://doi.org/10.1007/s00542-018-4081-1

[22] Khan, Najeeb Alam, Sidra Khan, and Fatima Riaz. "Boundary layer flow of Williamson fluid with chemically reactive species using scaling transformation and homotopy analysis method." *Mathematical Sciences Letters* 3, no. 3 (2014): 199. https://doi.org/10.12785/msl/030311

[23] Reddy, Y. Dharmendar, Fateh Mebarek-Oudina, B. Shankar Goud, and A. I. Ismail. "Radiation, velocity and thermal slips effect toward MHD boundary layer flow through heat and mass transport of Williamson nanofluid with porous medium." *Arabian Journal for Science and Engineering* 47, no. 12 (2022): 16355-16369. https://doi.org/10.1007/s13369-022-06825-2

[24] Li, Yi-Xia, Mohammed Hamed Alshbool, Yu-Pei Lv, Ilyas Khan, M. Riaz Khan, and Alibek Issakhov. "Heat and mass transfer in MHD Williamson nanofluid flow over an exponentially porous stretching surface." *Case Studies in Thermal Engineering* 26 (2021): 100975. https://doi.org/10.1016/j.csite.2021.100975

[25] Abbas, Amir, Mdi Begum Jeelani, Abeer S. Alnahdi, and Asifa Ilyas. "MHD Williamson nanofluid fluid flow and heat transfer past a non-linear stretching sheet implanted in a porous medium: Effects of heat generation and viscous dissipation." *Processes* 10, no. 6 (2022): 1221. https://doi.org/10.3390/pr10061221

[26] Hayat, T., M. Farooq, A. Alsaedi, and Z. Iqbal. "Melting heat transfer in the stagnation point flow of Powell-Eyring fluid." *Journal of Thermophysics and Heat Transfer* 27, no. 4 (2013): 761-766. https://doi.org/10.2514/1.T4059

[27] Dadheech, Amit, Amit Parmar, and Amala Olkha. "Inclined MHD and radiative Maxwell slip fluid flow and heat transfer due to permeable melting surface with a Non-linear heat source." *International Journal of Applied and Computational Mathematics* 7, no. 3 (2021): 89. https://doi.org/10.1007/s40819-021-01021-6

[28] Sharma, Surbhi, Amit Dadheech, Amit Parmar, Jyoti Arora, Qasem Al-Mdallal, and S. Saranya. "MHD micro polar fluid flow over a stretching surface with melting and slip effect." *Scientific Reports* 13, no. 1 (2023): 10715. https://doi.org/10.1038/s41598-023-36988-3

[29] Mabood, F., A. Shafiq, T. Hayat, and S. Abelman. "Radiation effects on stagnation point flow with melting heat transfer and second order slip." *Results in Physics* 7 (2017): 31-42. https://doi.org/10.1016/j.rinp.2016.11.051

[30] Khan, Muhammad Naveed, Shafiq Ahmad, Zhentao Wang, Bandar M. Fadhl, Kashif Irshad, Sayed M. Eldin, Amjad Ali Pasha, Mohammed K. Al Mesfer, and Mohd Danish. "Enhancement in the efficiency of heat recovery in a Williamson hybrid nanofluid over a vertically thin needle with entropy generation." *Heliyon* (2023): e17665. https://doi.org/10.1016/j.heliyon.2023.e17665

[31] Goud, B. Shankar. "Heat generation/absorption influence on steady stretched permeable surface on MHD flow of a micropolar fluid through a porous medium in the presence of variable suction/injection." *International Journal of Thermofluids* 7 (2020): 100044. https://doi.org/10.1016/j.ijft.2020.100044

[32] Amar, N., N. Kishan, and B. Shankar Goud. "Viscous dissipation and radiation effects on MHD heat transfer flow of Casson fluid through a moving wedge with convective boundary condition in the existence of internal heat generation/absorption." *Journal of Nanofluids* 12, no. 3 (2023): 643-651. https://doi.org/10.1166/jon.2023.1948

[33] Jalili, Payam, Ali Ahmadi Azar, Bahram Jalili, and Davood Domiri Ganji. "Study of nonlinear radiative heat transfer with magnetic field for non-Newtonian Casson fluid flow in a porous medium." *Results in Physics* 48 (2023): 106371. https://doi.org/10.1016/j.rinp.2023.106371

[34] Ramanuja, Mani, J. Kavitha, A. Sudhakar, A. Ajay Babu, Hari Kamala Sree, and K. Ramesh Babu. "Effect of Chemically Reactive Nanofluid Flowing Across Horizontal Cylinder: Numerical Solution." *Journal of Advanced Research in Numerical Heat Transfer* 12, no. 1 (2023): 1-17.

[35] Bakar, Shahirah Abu, Norihan Md Arifin, and Ioan Pop. "Stability Analysis on Mixed Convection Nanofluid Flow in a Permeable Porous Medium with Radiation and Internal Heat Generation." *Journal of Advanced Research in Micro and Nano Engineering* 13, no. 1 (2023): 1-17. https://doi.org/10.37934/armne.13.1.117